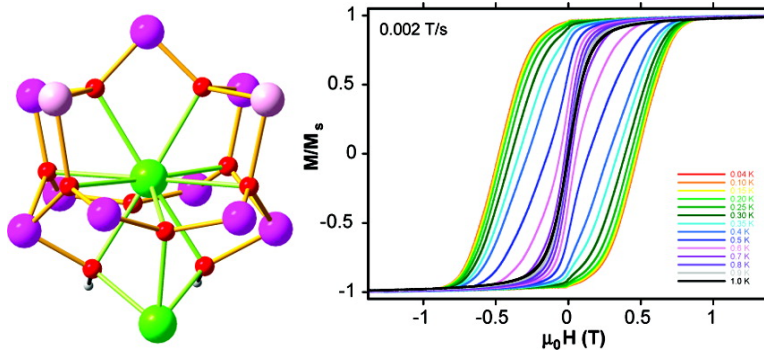


A Bell-Shaped MnGd Single-Molecule Magnet

Valeriu M. Mereacre, Ayuk M. Ako, Rodolphe Clrac, Wolfgang Wernsdorfer,
 George Filoti, Juan Bartolom, Christopher E. Anson, and Annie K. Powell

J. Am. Chem. Soc., **2007**, 129 (30), 9248-9249 • DOI: 10.1021/ja071073m • Publication Date (Web): 11 July 2007

Downloaded from <http://pubs.acs.org> on February 16, 2009



More About This Article

Additional resources and features associated with this article are available within the HTML version:

- Supporting Information
- Links to the 24 articles that cite this article, as of the time of this article download
- Access to high resolution figures
- Links to articles and content related to this article
- Copyright permission to reproduce figures and/or text from this article

[View the Full Text HTML](#)

A Bell-Shaped Mn₁₁Gd₂ Single-Molecule Magnet

Valeriu M. Mereacre,[†] Ayuk M. Ako,[†] Rodolphe Clérac,[‡] Wolfgang Wernsdorfer,[§] George Filoti,[#] Juan Bartolomé,[#] Christopher E. Anson,[†] and Annie K. Powell^{*†}

Institut für Anorganische Chemie der Universität Karlsruhe, D-76128 Karlsruhe, Germany, Université Bordeaux 1, CNRS, Centre de Recherche Paul Pascal—UPR8641, 115 avenue du Dr. Albert Schweitzer, 33600 Pessac, France, Institut Néel—CNRS, 38042 Grenoble Cedex 9, France, and Instituto de Ciencia de Materiales de Aragon, Ciuda Universitaria, 50009-Zaragoza, Spain

Received February 14, 2007; E-mail: powell@aoc.uni-karlsruhe.de

The synthesis of transition-metal clusters with unusual magnetic properties has become an area of intense research activity since the discovery of single-molecule magnets (SMMs).¹ The quest for new SMMs displaying high blocking temperatures has focused mainly on the use of paramagnetic 3d metal ions.^{2–5} SMM behavior results from the favorable arrangement of metal ions with single ion anisotropy in a high-ground-spin state molecule, and some recent synthetic efforts have turned attention to combining 3d and 4f ions in complexes to enhance both spin and anisotropy. Recent success in synthesizing mixed transition metal and lanthanide SMMs presenting various core topologies includes Cu₂Tb₂⁶ and Mn₆Dy₆,⁷ which have been described as SMMs on the observation of frequency-dependent out-of-phase *ac* signals, and Mn₁₁Dy₄,⁸ Mn₂Dy₂,⁹ Fe₂Dy₂,¹⁰ and Fe₂Ho₂,¹⁰ which additionally show hysteresis loops in the magnetization.

Recently we reported on triangular dysprosium compounds showing SMM behavior of thermally excited spin states¹¹ which has attracted us to exploring mixed d/f compounds as a means of enhancing anisotropy and/or spin state. Herein we report an efficient procedure toward the isolation of high-nuclearity heterometallic complexes using a preformed hexanuclear Mn complex, [Mn^{III}₂Mn^{II}₄O₂(piv)₁₀(4-Me-py)_{2.5}(pivH)_{1.5}]¹² (**1**) (pivH = 'BuCO₂H), as a source of Mn^{III} ions. Reaction of **1** with Gd(NO₃)₃·6H₂O in the presence of 2-furan-carboxylic acid (fcaH) in CH₃CN results in the formation of the high-nuclearity complex [Mn^{III}₉Mn^{II}₂Gd₂(O)₈(OH)₂(piv)_{10.6}(fca)_{6.4}(NO₃)₂(H₂O)]·13CH₃CN·H₂O (**2**·13MeCN·H₂O).¹³

The Mn₁₁Gd₂ aggregate **2** crystallizes¹⁴ in the triclinic space group *P* $\bar{1}$, and its molecular structure is shown in Figure 1. The oxidation states of the Mn centers were determined by bond-valence sum (BVS) calculations,¹⁵ with Mn(1)–Mn(9) assigned as Mn^{III} and Mn(10) and Mn(11) as Mn^{II}. The assignments of O(10) as (μ_3 -O)²⁻ and of O(2) and O(3) as (μ_3 -OH)⁻ were also confirmed by BVS calculations; the H-atoms on O(2) and O(3) could be located and refined. The core of the complex **2** can be described as bell-shaped. The Mn^{III} and Mn^{II} centers form the shell of the bell, with Mn(9) at the apex, Mn(5), Mn(8), Mn(10), and Mn(11) at the shoulder of the bell, and the remaining six Mn^{III} centers forming the rim of the bell. The two Gd centers can be thought of as forming the bell's clapper, and since the Gd···Gd vector is inclined with respect to the axis of the bell, this gives the impression that the bell is ringing. Gd(1) is ten-coordinate and is connected to each of the eleven Mn atoms through the six (μ_4 -O), one (μ_3 -O), and two (μ_3 -OH) bridges. Its coordination polyhedron may be best described as a bicapped square antiprism. The second Gd is nine-

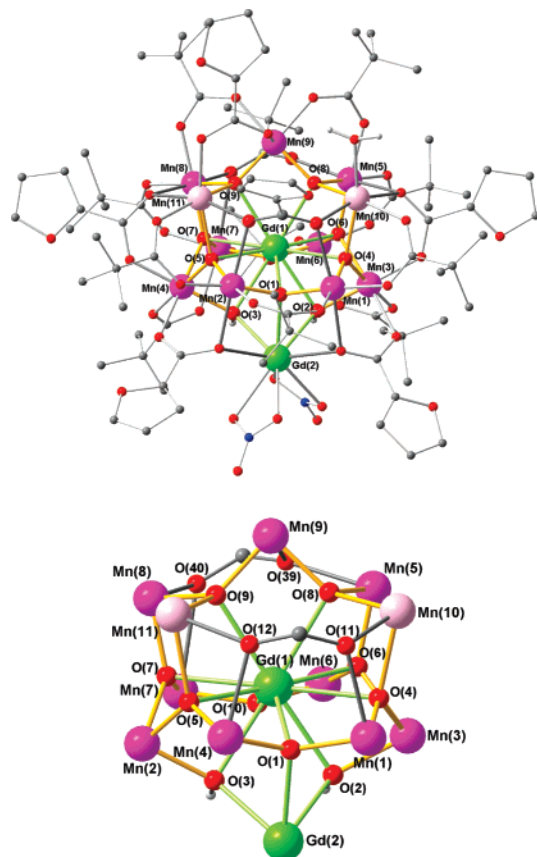


Figure 1. Molecular structure of **2** (above) and its core (below). Disorder and organic H-atoms omitted for clarity: Gd, green; Mn^{III}, purple; Mn^{II}, pink; O, red; N, blue; C, gray.

coordinate and hangs below the rim of the bell. It is connected to the other Gd and four of the Mn^{III} atoms through one (μ_4 -O) and the two (μ_3 -OH) bridges, and two oxygen atoms from two (μ_3 -carboxylate) bridges. Its coordination sphere is completed by two chelating nitrate ions. The Mn centers all have octahedral coordination geometries except for Mn(6), which is square-pyramidal, with the Mn^{III} all showing the expected Jahn–Teller distortions. Of the 17 carboxylate ligands (ten pivalate, six furoate, and one that is a disordered superposition), the unusual (μ_4, η^2, η^2) bridging mode is seen for one furoate and one pivalate ligand. In addition to these μ_4 -bridging carboxylates, four of the furoates adopt a (μ_3, η^2, η^1) triply bridging mode, while the sixth furoate and all the remaining pivalates form simple bridges between two metal centers. In other words, five of the six furoates bridge between three or four metal centers, whereas all but one of the pivalates adopt a simple μ_2 -bridging mode. The Mn^{III} Jahn–Teller axes have an irregular

[†] Universität Karlsruhe.

[‡] Université Bordeaux 1; CNRS, Centre de Recherche Paul Pascal.

[§] Institut Néel – CNRS.

[#] Instituto de Ciencia de Materiales de Aragon.

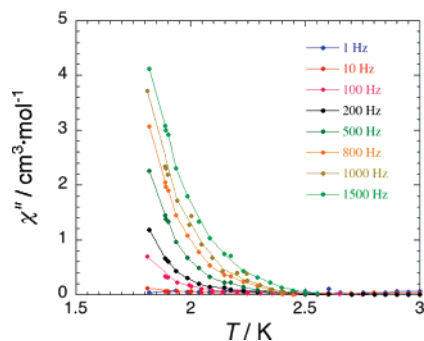


Figure 2. Plots of the out-of-phase (χ'') ac susceptibility signals versus temperature for complex **2** with an applied 3 Oe ac field in zero dc field.

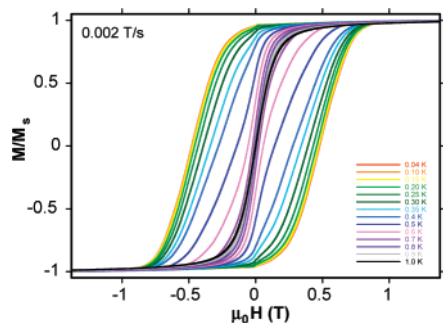


Figure 3. Magnetization (M) versus applied dc field ($\mu_0 H$) for **2**.

arrangement within the aggregate core (Figure S1). In addition to the bell-shaped core topology, **2** is the first mixed-valence Mn^{II,III}-Ln^{III} d/f complex and only the second synthesized Mn-Ln cluster with as many as eleven Mn centers.⁸

The dc magnetic susceptibility of **2** measured at 1000 Oe in the 1.8–300 K temperature range, reveals a room temperature χT value per complex of 46.9 cm³ K/mol. On lowering the temperature, χT first continuously decreases reaching 35.2 cm³ K/mol at 37 K and then increases to a maximum value at 1.81 K of 74.5 cm³ K/mol. The fact that the χT product starts to saturate at 1.81 K suggests that below this temperature a well-defined high-spin ground state is almost exclusively thermally populated (Figure S2). The fit of the experimental data to a Curie Weiss law above 30 K (Figure S3) leads to a Curie constant of 50.8 cm³ K/mol and a Weiss constant of –28.1 K indicating dominant antiferromagnetic interactions between spin carriers. The Curie constant is close to the expected value for nine Mn^{III} ($S = 2$), two Mn^{II} ($S = 5/2$) and two Gd^{III} ($S = 7/2$) noninteracting ions (51.5 cm³ K/mol).

The ac susceptibility measurements taken over the frequency range 1–1500 Hz and at temperatures of 1.8–3 K display frequency-dependent out-of-phase signals (Figure 2) suggesting that the complex exhibits slow relaxation of its magnetization and potential SMM behavior. To investigate this further, single-crystal magnetization measurements were performed using an array of micro-SQUIDS at temperatures down to 40 mK.¹⁶ Hysteresis loops collected for complex **2** at varying temperatures and sweep rates (Figure 3) show a superparamagnet-like increasing coercivity with decreasing temperature confirming **2** to be a SMM. No steps due to quantum tunneling of magnetization (QTM) were observed, probably as a result of ligand and lattice solvent disorder, as there are no obvious pathways for intermolecular interactions. The dc magnetization decay data were collected in the 0.04–1.0 K range: at each temperature, the magnetization was saturated with a dc field,

the temperature lowered to a chosen value, the field switched off, and the decay monitored with time. The data were scaled in a single master curve to construct the Arrhenius plot, and the fit of the thermally activated region above ~ 0.5 K gave $\tau_0 = 2 \times 10^{-12}$ s and an effective barrier $\Delta_{\text{eff}} = 18.4$ K, which is the highest value reported so far for 3d-4f SMMs.^{8,9} Given the lack of obvious intermolecular interactions, the relatively low value of τ_0 compared with other 3d-4f SMMs might be the result of the presence of a higher spin state. Below ~ 0.16 K, the relaxation time becomes essentially temperature-independent, consistent with the purely quantum regime where QTM is only via the lowest energy $\pm m_s$ levels. Probably the Jahn–Teller distortions of the Mn^{III} centers make the major contribution to the anisotropy with the Mn^{II} and Gd^{III} centers contributing to the spin.

In conclusion, this tridecanuclear manganese–lanthanide complex has an unusual topology and SMM properties. The synthetic method allows for the assembly of related materials.

Acknowledgment. We thank MAGMANet (NMP3-CT-2005-515767), Bordeaux 1 University, the CNRS, the Region Aquitaine, and the Alexander von Humboldt Foundation (V.M.).

Supporting Information Available: Crystallographic details in CIF format, experimental details, and magnetic data. This material is available free of charge via the Internet at <http://pubs.acs.org>.

References

- (1) (a) Sessoli, R.; Tsai, H.-L.; Schake, A. R.; Wang, S.; Vincent, J. B.; Foltig, K.; Gatteschi, D.; Christou, G.; Hendrickson, D. N. *J. Am. Chem. Soc.* **1993**, *115*, 1804. (b) Sessoli, R.; Gatteschi, D.; Caneschi, A.; Novak, M. A. *Nature* **1993**, *365*, 141.
- (2) (a) Price, J. P.; Batten, S. R.; Moubaraki, B.; Murray, K. S. *Chem. Commun.* **2002**, 762. (b) Sanudo, E. C.; Wernsdorfer, W.; Abboud, K. A.; Christou, G. *Inorg. Chem.* **2004**, *43*, 4137. (c) Coronado, E.; Forment-Aliaga, A.; Gaita-Arino, A.; Gimenez-Saiz, C.; Romero, F. M.; Wernsdorfer, W. *Angew. Chem., Int. Ed.* **2004**, *45*, 6152. (d) Maheswaran, S.; Chastanet, G.; Teat, S. J.; Mallah, T.; Sessoli, R.; Wernsdorfer, W.; Wippeny, R. E. P. *Angew. Chem.* **2005**, *117*, 5172.
- (3) Delfs, C.; Gatteschi, D.; Pardi, L.; Sessoli, R.; Wieghardt, K.; Hanke, D. *Inorg. Chem.* **1993**, *32*, 3099.
- (4) Cadiou, C.; Murrie, M.; Paulsen, C.; Villar, V.; Wernsdorfer, W.; Wippeny, R. E. P. *Chem. Commun.* **2001**, 2666.
- (5) (a) Yang, E.-C.; Hendrickson, D. N.; Wernsdorfer, W.; Nakano, M.; Zakharov, L. N.; Sommer, R. D.; Rheingold, A. L.; Ledezma-Gairaud, M.; Christou, G. *J. Appl. Phys.* **2002**, *91*, 7382. (b) Murrie, M.; Teat, S. J.; Stoeckli-Evans, H.; Gudel, H. U. *Angew. Chem.* **2003**, *115*, 4801; *Angew. Chem., Int. Ed.* **2003**, *42*, 4653.
- (6) Osa, S.; Kido, T.; Matsumoto, N.; Re, N.; Pochaba, A.; Mrozinski, J. J. *J. Am. Chem. Soc.* **2004**, *126*, 420.
- (7) Zaleski, C.; Depperman, E.; Kampf, J.; Kirk, M.; Pecoraro, V. *Angew. Chem., Int. Ed.* **2004**, *43*, 3912.
- (8) Mishra, A.; Wernsdorfer, W.; Abboud, K.; Christou, G. *J. Am. Chem. Soc.* **2004**, *126*, 15648.
- (9) Mishra, A.; Wernsdorfer, W.; Parson, S.; Christou, G.; Brechin, E. *Chem. Commun.* **2005**, 2086.
- (10) Murugesu, M.; Mishra, A.; Wernsdorfer, W.; Abboud, K.; Christou, G. *Polyhedron* **2006**, *26*, 613.
- (11) Tang, J.; Hewitt, I.; Madhu, N. T.; Chastanet, G.; Wernsdorfer, W.; Anson, C. E.; Benelli, C.; Sessoli, R.; Powell, A. K. *Angew. Chem.* **2006**, *118*, 1761.
- (12) See Supporting Information.
- (13) Anal. Found (calcd for $2 \cdot \text{CH}_3\text{CN} \cdot \text{H}_2\text{O}$): C, 34.39 (34.12); H, 4.21 (4.00); N, 1.19 (1.37).
- (14) Crystal data for $2 \cdot 13\text{CH}_3\text{CN} \cdot \text{H}_2\text{O}$: $\text{C}_{111}\text{H}_{157.6}\text{Gd}_2\text{Mn}_{11}\text{N}_{20}\text{O}_{58.4}$, 3555.36 g mol⁻¹, triclinic, $P1$, $a = 15.8893(10)$ Å, $b = 17.5285(11)$ Å, $c = 27.2474(17)$ Å, $\alpha = 86.985(1)^\circ$, $\beta = 78.083(1)^\circ$, $\gamma = 72.737(1)^\circ$, $Z = 2$, $V = 7090.5(8)$ Å³, $T = 100$ K, $\rho_{\text{calcd}} = 1.665$ g cm⁻³, $F(000) = 3598$, μ -(Mo K α) = 1.957 mm⁻¹; $2\theta_{\text{max}} = 52.7^\circ$, 33399 data, 28136 unique ($R_{\text{int}} = 0.0246$), 1408 parameters, final $wR_2 = 0.0907$, $S = 0.992$ (all data), R_1 (18636 data with $I > 2\sigma(I)$) = 0.0409. See Supporting Information for refinement details; CCDC 637050.
- (15) Liu, W.; Thorp, H. H. *Inorg. Chem.*, **1993**, *32*, 4102. Calculated values: Mn(1)–Mn(9) 2.82–2.94, Mn(10) 2.01, Mn(11) 1.91; O(1) and O(4)–O(10) 1.85–1.96, O(2) 1.18, O(3) 1.28.
- (16) Wernsdorfer, W. *Adv. Chem. Phys.* **2001**, *118*, 99.

JA071073M